Amplitude Shift Keying Constellation Space for Simultaneous Wireless Information and Power Transfer

Adnan Hanif
The George Washington University, Washington D.C.
adnanhanif@gwu.edu

Miloš Doroslovački
The George Washington University, Washington D.C.
doroslov@gwu.edu

***Abstract*—Simultaneous wireless information and power transfer (SWIPT) has the potential to realize the envisioned ubiquity of the internet of things (IoT) by energizing them wirelessly whilst exchanging information. Recently, low-complexity receiver architectures for SWIPT are being considered for decoding information from amplitude modulated signals after rectification. However, less attention is paid towards improving the non-linear rectifier model prevalent in these architectures which is often truncated till fourth-order term in diode characteristic. In this paper, a novel, tractable analytical model for the rectenna non-linearity is presented which provides a theoretical upper bound to harvested DC power over the amplitude shift keying (ASK) constellation space corresponding to the entire diode non-linear region. Besides, the work also exposes the convexity of harvested DC power vis-à-vis incoming signal power thereby verifying the rate-energy (R-E) tradeoff in SWIPT for different choices of transmitted symbol amplitude distributions. Finally, the theoretical results presented using the adopted model are substantiated with the Monte Carlo circuit simulations allowing to conveniently evaluate and draw compromise in SWIPT performance against a choice of modulation scheme out of the ASK constellation space.**

***Keywords*—Non-linear model, rectenna, amplitude shift keying, constellation space, modulation schemes, SWIPT.**

I. Introduction

The proliferation of the internet of things (IoT) in high-speed networks is one of the key enablers of widespread remote monitoring in smart cities, farmlands, industrial plants, etc. [1]. However, the massive expansion of these always-connected wireless devices presents an imminent challenge to power them in the long term especially when they are battery-limited or inaccessible [2]. This calls for a paradigm shift in future wireless sensor networks (WSN) design to meet their information as well as energy demands simultaneously [3]. Traditionally, radio frequency (RF) waves are mainly used for wireless information transfer (WIT) but, they can carry both energy and information. In the past few years, a continuing trend towards low-powered electronics and smart devices has paved a way for far-field wireless power transfer (WPT) using RF waves [4], [5]. This trend towards low energy-consuming devices will continue further and as per Koomey's law [6], in 20 years, the amount of energy required to compute a given task will fall by a factor of 10,000 compared to what it is today. The WPT presents a promising energy source by enabling long-distance, on-demand, and predictable power delivery to mobile wireless receivers which can be realized in a small form-factor compared to traditional magnetic resonance or inductive coupling technologies. Furthermore, the integration of WPT with WIT has the potential to make the best use of network infrastructure and RF spectrum to communicate and energize simultaneously [7].

Simultaneous wireless information and power transfer (SWIPT) first introduced in [8] refers to simultaneous WIT and WPT from base station transmitter to low-powered receivers, typical in IoT infrastructure. The design of an efficient SWIPT relies on the design of efficient WIPT which increases Direct-Current (DC) power at the harvester output [9]. The heart of the harvester is a rectenna which is made of an antenna attached to a non-linear device such as a diode followed by a low-pass filter to extract DC power from an incoming RF signal. Due to this non-linear nature of rectenna, [10]–[14] showed that the amount of harvested DC power is not only a function of rectenna design and signal power but is also a function of signal shape. In [12] and subsequent works, a simple rectenna model based on diode non-linearity is presented by Taylor series expansion of diode characteristic truncated up to fourth-order terms. This non-linearity is later exploited to improve RF-to-DC power conversion efficiency using transmit diversity [15] or using energy modulation [16]. Since many traditional WPT technologies consider information decoder (ID) and energy harvester (EH) as structurally separate architectures, the impact of system performance in terms of rate-energy (R-E) tradeoff is in focus [13], [14]. Similarly, the time-switching (TS) and power-splitting (PS) schemes based architectures suffer from complex designs and high energy-consuming RF components in addition to significant R-E tradeoffs which are often not practical for simple IoT devices [17].

To avoid splitting of the RF signal in terms of time or power, an integrated EH and ID receiver (IntRx) architecture proposed in [18] has come into focus. In IntRx design, a complete incoming RF signal is first rectified into a DC output which is followed by information decoding using rectified signals' amplitudes. Since the rectifying process is similar to envelop detection, receiver does not require energy-consuming RF components for conventional RF to baseband down-conversion making it suitable for low-power IoT devices. Various amplitude-inspired modulation techniques involving IntRx architecture for SWIPT exist [18]–[20]. Authors in [18] proposed a pulse energy modulation (PEM) for information decoding by employing an amplitude-shift keying (ASK) demodulation on the rectified DC signal over a double-sided constellation. Similarly, IntRx comprised of multiple antenna-rectifier pairs is used in [19] to deliver information via amplitude pattern for each pair. Recently, pulse position modulation (PPM) is used to maximize power transfer while delivering information through rectified DC pulse positions [20]. All these approaches attempt to make use of signal amplitude's constellation space to transfer information, however the relationship between such amplitude space with an upper bound of harvested DC power is not examined from the perspective of the rectenna model over its entire non-linear region.

In this paper, we propose a novel and tractable model of rectenna non-linearity for SWIPT. First, an analytical model is presented which provides a simple upper bound relationship to harvested DC of incoming amplitude modulated single-carrier signal without discarding higher-order terms in the Taylor series expansion of the diode characteristic. The model provides a direct insight into the choice of symbols for amplitude shift keying (ASK) out of the real constellation space which can maximize either information or power transfer, thereby highlighting the rate-energy tradeoff present in SWIPT. Next, the convexity of harvested DC power as a function of incoming signal power is exposed which favors signals with large peak-to-average power ratio (PAPR) for increasing harvested DC power inside the diode's non-linear region. Thus, the presented non-linear rectenna model provides convenient guidance to design and analyze future amplitude-inspired modulation schemes for optimal SWIPT performance from a spectrum of amplitude's constellation space. Finally, the theoretical results are corroborated with Monte Carlo circuit simulations which reiterate the tradeoff present in SWIPT receivers including power-splitting and time-sharing architectures that information is maximized for inputs with Gaussian-distributed signal amplitude and power is maximized for inputs with on-off keying (OOK) signal amplitude.

The rest of the paper is organized as follows: the novel non-linear system model is proposed in Section II, simulation results and discussion are provided in Section III, and finally, the conclusion is presented in Section IV.

II. Proposed System Model

In this section, a point-to-point SWIPT system model is considered with the receiver simultaneously decoding information and harvesting energy. Both transmitter and receiver achieve this using a single antenna to transfer information and energy simultaneously from the source to the receiver.

A. Signal Model

First, consider a generic N-carrier transmission having channel input $x(t)$ as,

$$x(t) = \Re\left\{\sum_{n=0}^{N-1} S_n e^{j2\pi f_n t}\right\}$$

where $S_n = A_n e^{j\phi_n}$ is complex amplitude with amplitude A_n and phase ϕ_n, of the n^{th}-carrier at frequency f_n and $f_n = f_o + n\Delta f, n = 0, .., N-1$. The input $x(t)$ is assumed a narrow-band signal with bandwidth B Hz and is subject to average transmit power constraint over all carriers. Here $B \ll f_n$ and $\Re\{\cdot\}$ denotes the real part of a complex signal. Next, the transmission is subject to AWGN channel. The transmitted signal $x(t)$ is then received at receiver as

$$z(t) = \Re\left\{\sum_{n=0}^{N-1} S_n e^{j2\pi f_n t}\right\} + w(t) \qquad (1)$$

where $w(t)$ is real white Gaussian noise with zero mean and variance ${\sigma_w}^2$. The transmit average power denoted $\mathrm{E}[P]$ thus constrains the average power available at the receiver, i.e., $\mathrm{E}[\mathcal{E}\{|z(t)|^2\}] = \mathrm{E}[P] + {\sigma_w}^2$, where $\mathcal{E}$ and E denote time-averaging and statistical expectation, respectively. In further consideration, the contribution of AWGN towards energy harvesting only is assumed small and thus can be ignored [3].

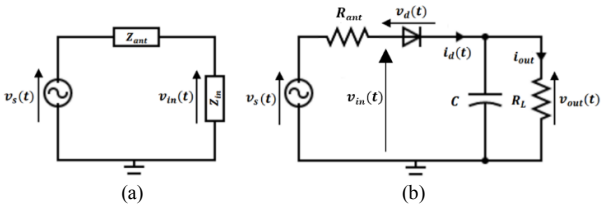

Fig. 1. (a) Rectenna equivalent circuit, (b) Single series diode antenna–rectifier circuit.

B. Rectenna Model

The rectifier–antenna model commonly referred to as rectenna represents the power transfer from the antenna to the rectifier through the matching network. Fig. 1 (a) illustrates an equivalent circuit of lossless antenna modeled as a voltage source $v_s(t)$ with antenna impedance $Z_{ant} = R_{ant} + jX_{ant}$ in series, where R_{ant} is antenna radiation resistance and X_{ant} is antenna radiation reactance. Similarly, the rectifier is modeled with impedance $Z_{in} = R_{in} + jX_{in}$. In the impedance matching case ($Z_{ant} = {Z_{in}}^*$), the rectifier resistance R_{in} completely absorbs the RF power available from the antenna P_{rf}, so that $P_{rf} = \mathrm{E}[\mathcal{E}\{|v_{in}(t)|^2\}]/R_{ant}$. Since $P_{rf} = \mathrm{E}[P]$, we have

$$v_{in}(t) = \frac{v_s(t)}{2} = z(t)\sqrt{R_{ant}}\,.$$

C. Non-linear Diode Model

Consider a simple rectifier circuit as shown in Fig. 1 (b) composed of a single diode in series with a low-pass filter containing load resistance R_L. Although this rectifier circuit is based on a single diode, it holds valid for more general rectifiers with many diodes [21]. As shown in Fig. 1 (b), the voltage drop across the diode $v_d(t) = v_{in}(t) - v_{out}(t)$, where $v_{in}(t)$ is the input voltage to diode and $v_{out}(t)$ is the output voltage across the resistor R_L.

Given a diode characteristic function,

$$i_d(t) = i_s\left(e^{v_d(t)/\eta v_t} - 1\right) = i_s\left(e^{v_{in}(t) - v_{out}(t)/\eta v_t} - 1\right) \quad (2)$$

where i_s is reverse bias saturation current, v_t is thermal voltage, and η is the diode ideality factor. Note that $i_d(t) > -i_s$ and so $\mathcal{E}\{i_d(t)\} > -i_s$. In (2), expressing $v_{in}(t)$ in terms of a sinusoidal source voltage $v_s(t)$ and assuming a steady-state response with an ideal low-pass filter, $v_{out}(t) \approx \mathcal{E}\{v_{out}(t)\} = \mathcal{E}\{i_d(t)\}R_L$, thus

$$i_d(t) = i_s\left(e^{v_s(t) - i_d(t)R_{ant} - \mathcal{E}\{i_d(t)\}R_L/\eta v_t} - 1\right)$$

or

$$\left(\frac{i_d(t)}{i_s} + 1\right) e^{\mathcal{E}\{i_d(t)\}R_L + i_d(t)R_{ant}/\eta v_t} = e^{v_s(t)/\eta v_t}. \quad (3)$$

Now taking time-average on both sides of (3) and invoking Jensen's inequality on l.h.s,

$$\left(\frac{i_d}{i_s} + 1\right) e^{i_d(R_L + R_{ant})/\eta v_t} \le \mathcal{E}\left\{e^{v_s(t)/\eta v_t}\right\}$$

where $i_d = \mathcal{E}\{i_d(t)\}$ is the time-averaged $i_d(t)$ which can possess statistical randomness depending upon the statistical randomness of the transmitted symbols S_n. For simplicity, we take single-tone sinusoid in (1) with $S = S_0 \in \mathbb{R}$, so

$$\left(\frac{i_d}{i_s}+1\right)e^{i_d(R_L+R_{ant})/\eta v_t} \le \mathcal{E}\left\{e^{2z(t)\sqrt{R_{ant}}/\eta v_t}\right\} = \mathcal{E}\left\{e^{2S\sin(2\pi f_0 t)\sqrt{R_{ant}}/\eta v_t}\right\}$$

which can be rewritten as

$$g(i_d) \le \frac{1}{2\pi}\int_{-\pi}^{\pi} e^{\rho\sin(\tau)}\,d\tau = \frac{1}{2\pi}\int_{-\pi}^{\pi} e^{\rho\sin(\tau)-j\nu\tau}\,d\tau\Big|_{\nu=0}$$

$$g(i_d) \le \frac{1}{2\pi}\int_{-\pi}^{\pi} e^{j(-j\rho\sin(\tau)-\nu\tau)}\,d\tau\Big|_{\nu=0} \quad (4)$$

where $g(i_d)$ is a convex function of i_d and $\rho = 2S\sqrt{R_{ant}}/(\eta v_t)$.

Now, expressing r.h.s of (4) as a Bessel function of the first kind, order zero $J_0(\cdot)$ and denoting $h(\cdot)$ as an inverse function of $g(\cdot)$ which is monotonically increasing and concave, (4) can be rewritten as,

$$i_d \le h\{J_0(-j\rho)\}. \quad (5)$$

Here the upper bound on i_d can be solved using a numerical approach to find the inverse function $h(\cdot)$, which can be expressed using Lambert W function [22]. Finally, squaring (5), the upper-bounded DC power of P_{dc} delivered to load R_L will be

$$P_{dc} = {i_d}^2 R_L \le [h\{J_0(-j\rho)\}]^2 R_L. \quad (6)$$

Eq (6) provides a novel tractable model depicting the relationship of signal amplitude to harvested DC power without truncation of higher-order statistics. Furthermore, with power P available per symbol for rectification in the case of the perfect antenna–rectifier impedance matching, the source voltage signal $v_s(t) = 2\sqrt{R_{ant}}z(t)$ has a peak amplitude $V_s = 2\sqrt{R_{ant}}|S| = \sqrt{8R_{ant}P}$. Thus, (6) leads to traditional analysis of harvested DC power P_{dc} for a given input power P which can also be well approximated by expressing (5) in terms of a higher-order polynomial as discussed in section III B.

D. Net Harvesting Efficiency

The non-linear diode model currently being adopted in SWIPT architectures which are truncated to fourth-order term accounts for the dependence of RF-to-DC power conversion efficiency $\eta = P_{dc}/P$ of the rectifier circuit on the input signal power [12]. Consistently, the upper-bounded non-linear diode model presented here theorize the significance of high symbol amplitude variability of input signal for increasing the net harvesting power efficiency,

$$\eta_{net} \triangleq \frac{\mathrm{E}[P_{dc}]}{\mathrm{E}[P]} \quad (7)$$

calculated with average output power over average available power. Since $P_{dc} = \eta P$ is the convex function of P [13], we can simply write

$$\mathrm{E}[P_{dc}(P)] \ge P_{dc}(\mathrm{E}[P])$$

due to Jensen's inequality. This implies that the net harvesting power efficiency η_{net} in (7) due to varying input power is greater or equal to the efficiency of a carrier due to fixed input power, i.e.

$$\eta_{net} = \frac{\mathrm{E}[P_{dc}(P)]}{\mathrm{E}[P]} \ge \frac{P_{dc}(\mathrm{E}[P])}{\mathrm{E}[P]}. \quad (8)$$

E. Information Transfer

We consider SWIPT schemes with N carriers over a deterministic channel where the received value for a transmitted amplitude symbol vector $\mathrm{S} = [S_0 \ldots S_{N-1}]$ is an output vector $\mathrm{Z} = [Z_0 \ldots Z_{N-1}]$. The corresponding mutual information is,

$$I(\mathbf{S};\mathbf{Z}) = NI(S_0;Z_0) \quad (9)$$

S_n being *i.i.d.* random variables, and the channel output for a single symbol $Z = S + W$ where $W \sim \mathcal{N}(0, {\sigma_w}^2)$ is the channel noise. Since the rectifier noise can be negligible, it is ignored in WIT calculations. Dropping the subscript in (9), the mutual information for a single symbol becomes,

$$I(S;Z) = H(Z) - \frac{1}{2}\log_2(\pi e {\sigma_w}^2) \quad (10)$$

where $H(Z) = -\int p_Z(z)\log_2\big(p_Z(z)\big)\,dz$ and the output density function is given as

$$p_Z(z) = \sum_{n=0}^{N-1} p_S(s_n)p_W(z-s_n).$$

From [23], (10) reach information capacity $\mathcal{C}$ when $H(Z)$ is maximized by transmitting Gaussian symbol amplitudes in each carrier, i.e., $S_n \sim \mathcal{N}(0, 2\mathrm{E}[P]/N)$.

III. Simulation Results and Discussion

First, we present the theoretical bound as well as simulation results for harvested DC over the entire symbol amplitude constellation on both sides of zero. Next, the polynomial approximation of the harvested DC in the constellation region is demonstrated. Lastly, the SWIPT performance is assessed under varying symbol amplitude distribution including capacity-achieving distribution through AWGN channel.

A. Setup

The circuit presented in Fig.1 (b) is simulated in Matlab to account for impedance mismatch between antenna and rectifier under varying power P available for rectification. The rectifying diode is implemented with Skyworks SMS7630 Schottky diode due to its low bias voltage requirement and with $i_s = 5\ \mu\mathrm{A}$, $\eta = 1.05$, and $v_t = 25.86\ \mathrm{mV}$. The optimized low-pass filter with $C = 4.8$ pF and load $R_L = 3\ \mathrm{K}\Omega$ is employed for single-tone 5.18 GHz carrier frequency having average input power $\mathrm{E}[P] = -20$ dBm and antenna resistance $R_{ant} = 50\ \Omega$. The model is concurrently simulated in NI Multisim with an impedance matching network, and using symbol amplitude S corresponding to $\sqrt{2P}$.

B. Harvested DC and its Polynomial approximation

We first evaluate the theoretical upper bound for harvested DC as presented in (5) over a range of symbol amplitudes S in symmetric constellation space providing up to 7 dBm power available. This range captures the entire non-linear region of the diode. Consequently, the dependence on S of inverse function of Bessel function of the first kind order zero, particularly $h\{J_0(-j\rho)\}$ where $\rho = 2\sqrt{R_{ant}}S/(\eta v_t)$ is presented by solving the inverse function using the interior point method. As demonstrated in Fig. 2, the relationship is linear for a large range of S. Next, the harvested DC i_d is simulated over the same constellation space and is shown in

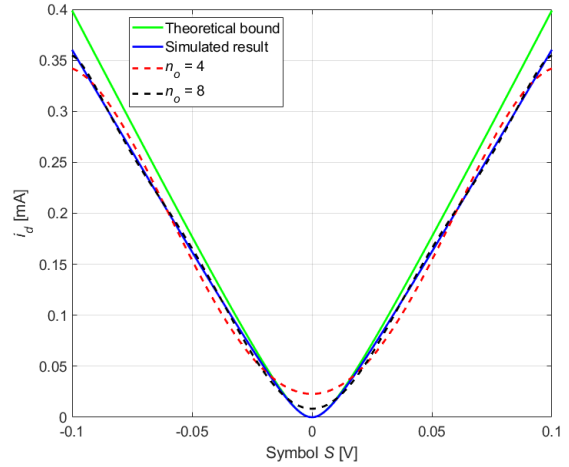

Fig. 2. Comparison of harvested DC i_d over amplitude's constellation space among theoretical upper bound, simulation, and approximation via polynomial of degree n_o.

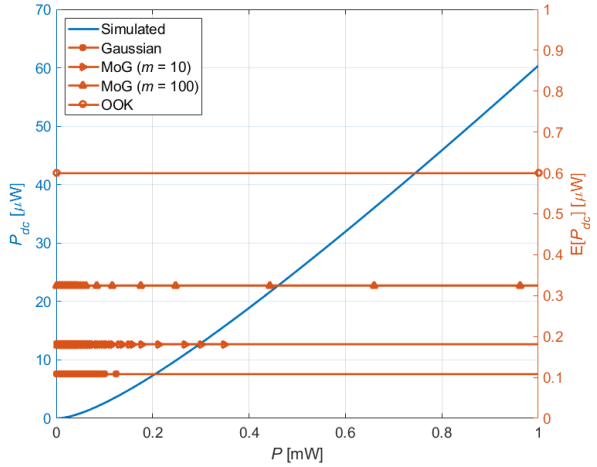

Fig. 3. Left-axis: Convexity of harvested DC power P_{dc} over P. Right-axis: Comparison of net harvested DC power $\mathrm{E}[P_{dc}]$ for fixed $\mathrm{E}[P] = -20$ dBm for Gaussian, a mixture of Gaussian, and OOK distributions.

Fig. 2 along with the theoretical upper bound. Fig. 2 depicts for the first time a clear visualization of the harvested DC relationship to symbol amplitude which can be used to design and evaluate the harvesting performance of an ASK modulation scheme from the entire real constellation space.

From the simulated-result plot in Fig. 2, it seems reasonable to approximate the result by using a closed-form polynomial equation. Particularly, the polynomial

$$p(S) = p_1 S^{n_o} + p_2 S^{n_o-1} + \cdots + p_{n_o} S + p_{n_o+1}$$

of symbol amplitude S of degree n_o which is the best fit in a least-square sense is evaluated for harvested DC i_d. Thus, Fig. 2 also depicts the plot of two polynomial fitted curves of degree $n_o = 4$ and $n_o = 8$ under setup conditions. Clearly, the polynomial of $n_o = 8$ is a better fit than that of $n_o = 4$. Note that they have zero coefficients for odd powers of S and non-zero coefficients for even powers of S. Assuming a probability distribution for S, the polynomial of degree n_o provides closed-form harvested DC output $i_{out} = \mathrm{E}[i_d] \approx \mathrm{E}[p(S)]$ which allows to conveniently choose the level of approximation required to evaluate ASK constellation points' performance.

C. SWIPT Performance in Constellation Space

The upper-bounded non-linear diode model presented in (6) is used to analyze the SWIPT performance in terms of net harvested DC power $\mathrm{E}[P_{dc}]$. Under average RF signal power $\mathrm{E}[P] = -20$ dBm , the results are simulated for three distributions of symbol amplitude S, namely a Gaussian, i.e., $S \sim \mathcal{N}(0, \sigma^2)$ for $\sigma^2 = 2\mathrm{E}[P]/N$, a mixture of Gaussian, i.e., $S \sim \mathcal{N}_1(0, \sigma_1^2)$ with probability p and $S \sim \mathcal{N}_2(0, \sigma_2^2)$ with probability $1-p$ where $\sigma_2^2 = m\sigma_1^2$ and $m \geq 1$ for $p\sigma_1^2 + (1-p)m\sigma_1^2 = 2\mathrm{E}[P]/N$, and an on-off keying (OOK), i.e., $|S| = \sqrt{2\mathrm{E}[P]/(Np')}$ with probability p' and $S = 0$ with probability $1-p'$.

For the considered WIT schemes, it is well established that Gaussian distribution reaches information capacity $\mathcal{C}$ in the presence of AWGN channel [23]. Generally, a mixture of Gaussian distributions with $m = 1$, $m = 10$, and $m = 100$ have an information rate $\mathcal{R}_m$ as per relation

$$\mathcal{C} = \mathcal{R}_1 > \mathcal{R}_{10} > \mathcal{R}_{100}.$$

However, for WPT performance, 1 million samples from these distributions result in an opposite trend of the net harvested DC power $\mathrm{E}[P_{dc}]$. As shown in Fig. 3 right axis, the Gaussian ($m = 1$) and the mixture of Gaussian ($m = 10,\ m = 100$) distributed symbols (shown with corresponding markers along P) result in net harvested DC power $\mathrm{E}[P_{dc}]_m$ as per relation

$$\mathrm{E}[P_{dc}]_{\mathrm{OOK}} > \mathrm{E}[P_{dc}]_{100} > \mathrm{E}[P_{dc}]_{10} > \mathrm{E}[P_{dc}]_1$$

where $E[P_{dc}]_{\mathrm{OOK}}$ is the net harvested DC power of OOK distribution. This trend is a direct consequence of the convexity of the harvesting output power P_{dc} as shown in Fig. 3 left axis. Moreover, it can also be inferred from Fig. 3 that the OOK distribution being a limiting case of a heavy-tailed distribution provides the maximum net harvested DC power $\mathrm{E}[P_{dc}]$ out of all input symbol amplitude distributions with an average power $\mathrm{E}[P]$. Therefore, the performance of SWIPT over the symbol amplitude's constellation space again highlights the R-E tradeoff where a particular choice of symbol amplitude distribution can maximize either power transfer or information rate.

IV. Conclusion

In this paper, we presented a tractable analytical relationship between harvested DC in SWIPT receivers and choice of transmitted symbol amplitude from ASK constellation space for the entire non-linear region of the diode. This is enabled by deriving a novel non-linear rectenna model without truncating any of the higher-order terms from the diode characteristic, thereby providing a theoretical upper bound on harvested DC power. We also highlighted the R-E tradeoff in SWIPT receivers by exposing the convexity of harvested DC power for incoming single-carrier signal power. The theoretical performance of SWIPT within the constellation space is contrasted with Monte Carlo circuit simulations. Both theoretical and simulation results demonstrate that the WPT rate is increased for higher PAPR symbol amplitude distributions with maximum achieved for OOK scheme, whereas the WIT rate achieves capacity for Gaussian distributed symbol amplitudes transmitted through AWGN channel under the same average transmit power constraint. Hence, the trade-off between WPT and WIT performance is verified for the presented non-linear rectenna model.

REFERENCES

[1] Y. Qian, D. Wu, W. Bao and P. Lorenz, "The Internet of Things for Smart Cities: Technologies and Applications," in *IEEE Network*, vol. 33, no. 2, pp. 4-5, March/April 2019.

[2] D. Kim, H. Lee, K. Kim and J. Lee, "Dual Amplitude Shift Keying with Double Half-Wave Rectifier for SWIPT," in *IEEE Wireless Communications Letters*, vol. 8, no. 4, pp. 1020-1023, Aug. 2019.

[3] B. Clerckx, R. Zhang, R. Schober, D. W. K. Ng, D. I. Kim and H. V. Poor, "Fundamentals of Wireless Information and Power Transfer: From RF Energy Harvester Models to Signal and System Designs," in *IEEE Journal on Selected Areas in Communications*, vol. 37, no. 1, pp. 4-33, Jan. 2019.

[4] J. R. Smith, "Wirelessly Powered Sensor Networks and Computational RFID," New York Springer, 2013.

[5] S. Hemour and K. Wu, "Radio-Frequency Rectifier for Electromagnetic Energy Harvesting: Development Path and Future Outlook," in *Proceedings of the IEEE*, vol. 102, no. 11, pp. 1667-1691, Nov. 2014.

[6] J. Koomey, S. Berard, M. Sanchez and H. Wong, "Implications of Historical Trends in the Electrical Efficiency of Computing," in *IEEE Annals of the History of Computing*, vol. 33, no. 3, pp. 46-54, March 2011.

[7] B. Clerckx, J. Kim, K. W. Choi and D. I. Kim, "Foundations of Wireless Information and Power Transfer: Theory, Prototypes, and Experiments," in *Proceedings of the IEEE*, vol. 110, no. 1, pp. 8-30, Jan. 2022.

[8] L. R. Varshney, "Transporting Information and Energy Simultaneously," *2008 IEEE International Symposium on Information Theory*, 2008, pp. 1612-1616.

[9] M. Varasteh, B. Rassouli and B. Clerckx, "Wireless information and power transfer over an AWGN channel: Nonlinearity and asymmetric Gaussian signaling," *2017 IEEE Information Theory Workshop (ITW)*, 2017, pp. 181-185.

[10] A. Collado and A. Georgiadis, "Optimal Waveforms for Efficient Wireless Power Transmission," in *IEEE Microwave and Wireless Components Letters*, vol. 24, no. 5, pp. 354-356, May 2014.

[11] C. R. Valenta, M. M. Morys and G. D. Durgin, "Theoretical Energy-Conversion Efficiency for Energy-Harvesting Circuits Under Power-Optimized Waveform Excitation," in *IEEE Transactions on Microwave Theory and Techniques*, vol. 63, no. 5, pp. 1758-1767, May 2015.

[12] B. Clerckx and E. Bayguzina, "Waveform Design for Wireless Power Transfer," in *IEEE Transactions on Signal Processing*, vol. 64, no. 23, pp. 6313-6328, 1 Dec.1, 2016.

[13] B. Clerckx, "Wireless Information and Power Transfer: Nonlinearity, Waveform Design, and Rate-Energy Tradeoff," in *IEEE Transactions on Signal Processing*, vol. 66, no. 4, pp. 847-862, 15 Feb.15, 2018.

[14] E. Bayguzina and B. Clerckx, "Modulation Design for Wireless Information and Power Transfer with Nonlinear Energy Harvester Modeling," *2018 IEEE 19th International Workshop on Signal Processing Advances in Wireless Communications (SPAWC)*, 2018, pp. 1-5.

[15] B. Clerckx and J. Kim, "On the Beneficial Roles of Fading and Transmit Diversity in Wireless Power Transfer With Nonlinear Energy Harvesting," in *IEEE Transactions on Wireless Communications*, vol. 17, no. 11, pp. 7731-7743, Nov. 2018.

[16] M. Varasteh, B. Rassouli and B. Clerckx, "On Capacity-Achieving Distributions for Complex AWGN Channels Under Nonlinear Power Constraints and Their Applications to SWIPT," in *IEEE Transactions on Information Theory*, vol. 66, no. 10, pp. 6488-6508, Oct. 2020.

[17] C. Im, J. Lee and C. Lee, "A Multi-Tone Amplitude Modulation Scheme for Wireless Information and Power Transfer," in *IEEE Transactions on Vehicular Technology*, vol. 69, no. 1, pp. 1147-1151, Jan. 2020.

[18] X. Zhou, R. Zhang and C. K. Ho, "Wireless Information and Power Transfer: Architecture Design and Rate-Energy Tradeoff," in *IEEE Transactions on Communications*, vol. 61, no. 11, pp. 4754-4767, Nov. 2013.

[19] R. Zhang, L. Yang and L. Hanzo, "Energy Pattern Aided Simultaneous Wireless Information and Power Transfer," in *IEEE Journal on Selected Areas in Communications*, vol. 33, no. 8, pp. 1492-1504, Aug. 2015.

[20] J. Kim and B. Clerckx, "Wireless Information and Power Transfer for IoT: Pulse Position Modulation, Integrated Receiver, and Experimental Validation," *arXiv:2104.08404*, 2021.

[21] B. Clerckx and E. Bayguzina, "Low-Complexity Adaptive Multisine Waveform Design for Wireless Power Transfer," in *IEEE Antennas and Wireless Propagation Letters*, vol. 16, pp. 2207-2210, 2017.

[22] I. Mező and Á. Baricz, "On the generalization of the Lambert *W* function," in *Transactions of the American Mathematical Society*, vol. 369, no. 11, pp.7917-7934, 2017.

[23] T. M. Cover and J. A. Thomas, *Elements of Information Theory*, 2nd ed., John Wiley & Sons, 2006.